PHYSICAL REVIEW C VOLUME 40, NUMBER 3 SEPTEMBER 1989

# Model analysis of the relationship between $^3S_1$ scattering length and the root-mean-square radius of the deuteron

W. van Dijk
*Redeemer College, Ancaster, Ontario, Canada L9G 3N6*
*and Physics Department, McMaster University, Hamilton, Ontario, Canada L8S 4M1*
(Received 13 March 1989)

By considering a number of nonrelativistic potential models, the relationship between the $^3S_1$ scattering length and the root-mean-square radius of the deuteron is studied. It is found that this relationship for certain classes of potentials is characterized by approximately straight line graphs similar to the one obtained by Klarsfeld *et al.* for a set of realistic nucleon-nucleon interactions. The implication of this study is that nonrelativistic nucleon-nucleon potentials of the types considered must include nonlocal components in order to be able to predict simultaneously the experimental triplet $S$-wave scattering length and the root-mean-square radius of the deuteron.

## I. INTRODUCTION

A number of nonrelativistic potential models give reasonable descriptions of the nucleon-nucleon interaction. Since these models are fitted to elastic scattering data and the deuteron properties, they are approximately equivalent on the energy shell, but because of the limited amount of additional data used in the fitting they lead to different off-shell properties of the transition matrix. In order to determine which of these potentials provides the most accurate description of the nuclear force, one needs to study physical properties that depend on the short- and medium-range behavior of the wave function.

In a precise comparison of certain low-energy properties predicted by a variety of realistic potentials, Klarsfeld *et al.*[1] found a severe constraint on the relationship between the triplet scattering length and the root-mean-square (rms) radius of the deuteron. The graph of the triplet scattering length as a function of the rms radius for various potentials is a straight line. (See Fig. 6 of Ref. 1.) Since this line, i.e., the $a_t - r_m$ relation, does not pass through the experimental region but below it, it appears that realistic nonrelativistic potentials are unable to fit within experimental error the triplet scattering length and the rms radius of the deuteron simultaneously.

Explanations for this discrepancy have been sought. Klarsfeld *et al.*[1] rule out meson-exchange-current effects, as they give corrections to the matter radius which increase rather than decrease the disagreement between potential models and experiment. Using one-dimensional models Toyama and Nogami[2] have investigated the effect on the scattering length and the rms radius when the Dirac equation rather than the Schrödinger equation is used as the fundamental equation of motion. They find that the same linear $a_t - r_m$ relation holds for both relativistic and nonrelativistic models. Hence they conclude that relativistic calculations will not give agreement with experiment. Although their analysis is limited to one-dimensional models, preliminary calculations with three-dimensional models using the Dirac equation with separable potentials and their phase equivalent nonrelativistic potentials lead to the same conclusions.[3]

Another possible avenue of investigation involves the quark and other exotic degrees of freedom in the nucleon-nucleon interaction. However, a prior question is whether within the framework of nonrelativistic potential models it is possible to find potentials whose scattering lengths and rms radii correspond to points that do not fall on the linear $a_t - r_m$ relation of Klarsfeld *et al.*[1] If such points are found, what characteristics do those potentials display that are different from the set of realistic potentials that yielded the results of Refs. 1 and 2?

In this paper several classes of potential models are considered, all of which have the same bound-state energy, namely, the deuteron energy. By varying some parameter, different members of a particular class of potentials are generated along with their scattering lengths and rms radii. In this way one obtains the $a_t - r_m$ relation for that class of potentials. Since Toyama and Nogami[2] suggest that the $a_t - r_m$ relation may be sensitive to the nonlocality of the potential, some of the potential models are constructed to have different degrees of nonlocal behavior. The results show indeed that the nonlocal potentials yield $a_t - r_m$ relations that are shifted in the right direction by sufficiently large amounts, so that potentially the discrepancy between experiment and theory can be resolved by including nonlocal parts in realistic interactions.

It must be pointed out that the calculations of this paper are model calculations. Higher-energy scattering phase shifts can be shown to vary significantly in these models, as is also noted in Ref. 2. One can, in principle, constrain the phase shifts to the experimental phases by employing more complex models, but that would not alter the qualitative conclusions of the nature of the $a_t - r_m$ relation. It should be noted that the $a_t - r_m$ relation from the analysis of realistic potentials by Klarsfeld *et al.*[1] and those obtained in this paper using much simpler models are very similar.

In Sec. II several classes of potentials are introduced to

 

compare their $a_t - r_m$ relations. The effect of $D$-state probability on this relation is also investigated. The consequences of several types of nonlocal potentials are analyzed in Sec. III. Section IV is a discussion of the results.

## II. SCATTERING LENGTHS AND rms RADII

In order to study the $a_t - r_m$ relation, model calculations with a variety of elementary interactions are performed. The interactions are chosen so that in many cases analytical expressions for the scattering length and rms radius are obtained.

### A. $S$-state interactions

For the $S$-state interactions the $l=0$ partial-wave Schrödinger equation is employed. The basis of orthonormal wave functions in the $S$ state is taken to be[4]

$$\langle p/r \rangle = \sqrt{2/\pi}\sin(pr) . \tag{2.1}$$

The normalized bound-state wave function is denoted by $u(r)$ in coordinate space and by

$$\tilde{u}(p) = \sqrt{2/\pi}\int_0^\infty \sin(pr)u(r)dr \tag{2.2}$$

in momentum space.

The scattering phase shift $\delta(k)$ is determined from the asymptotic form of the scattering wave function in coordinate space $u(k,r)$, where $k^2$ is the center-of-mass energy of the system. Thus as $r \to \infty$,

$$u(k,r) \sim \sqrt{2/\pi}\sin(kr+\delta) . \tag{2.3}$$

At low energy an effective range expansion holds; in the $S$ state it is

$$k\cot\delta(k) = -\frac{1}{a_t} + \frac{1}{2}r_t k^2 + \cdots , \tag{2.4}$$

where $a_t$ is the scattering length and $r_t$ the effective range.

The rms radius of the bound state is denoted by $r_m$, where

$$r_m^2 = \tfrac{1}{4}\langle r^2 \rangle = \tfrac{1}{4}\int_0^\infty r^2 u^2(r)dr , \tag{2.5}$$

and where $u$ is normalized to unity. When the bound-state wave function is found in the momentum representation, e.g., for separable potentials, it is easier to employ a relation equivalent to Eq. (2.5), namely,

$$r_m^2 = \tfrac{1}{4}\int_0^\infty \left[\frac{d\tilde{u}}{dp}\right]^2 dp . \tag{2.6}$$

In the remainder of this subsection a number of potentials acting only in the $S$ state are introduced. These models have different characteristics in terms of local and nonlocal properties, incorporation of the hard core, and the manner in which the potential goes to zero as the nucleon-nucleon separation distance increases.

#### 1. *Separable effective range interaction*

A nonlocal potential of the separable type giving the two-term effective range formula exactly in momentum space is[5]

$$V(p,p') = -\lambda_1 v(p)v(p') , \tag{2.7}$$

where

$$v(p) = \frac{p\gamma}{(p^2+\gamma^2)^{1/2}} . \tag{2.8}$$

The scattering length is given by the expression

$$a_t = \frac{1}{\gamma - 2/(\pi\lambda_1)} . \tag{2.9}$$

The condition that the potential of Eqs. (2.7) and (2.8) support a bound state is

$$\alpha = -\gamma + \tfrac{1}{2}\pi\lambda_1\gamma^2 > 0 , \tag{2.10}$$

where $\alpha^2$ is the binding energy. The scattering length may be written in terms of $\alpha$ and $\gamma$, so that

$$a_t = \frac{\alpha+\gamma}{\alpha\gamma} . \tag{2.11}$$

Using the bound-state wave function in momentum space, one obtains the rms radius in terms of an integral,

$$r_m^2 = \frac{\alpha}{\pi}(\alpha+\gamma)^2\int_0^\infty \frac{(-2p^4-p^2\gamma^2+\gamma^2\alpha^2)^2}{(p^2+\gamma^2)^3(p^2+\alpha^2)^4}dp . \tag{2.12}$$

Throughout this paper the numerical value $\alpha$ is fixed by the deuteron bound-state energy; i.e., $\alpha = 0.2316$ fm$^{-1}$. The relationship between the scattering length and the rms radius may be studied by using Eqs. (2.11) and (2.12), i.e., by calculating these quantities for different values of $\gamma$.

#### 2. *Yamaguchi potential*

The Yamaguchi potential[6] has the form of Eq. (2.7) with the form factor

$$v(p) = \frac{p\beta^2}{p^2+\beta^2} . \tag{2.13}$$

Its scattering length is known analytically as

$$a_t = \frac{2\pi\lambda_1}{\pi\lambda_1\beta - 4} . \tag{2.14}$$

There is one bound state when

$$\alpha = -\beta + \frac{\beta}{2}\sqrt{\pi\lambda_1\beta} > 0 . \tag{2.15}$$

This condition is used to determine $\lambda_1$ for a given value of $\beta$. The bound-state wave function in coordinate space has a simple form

$$u(r) = N(e^{-\alpha r} - e^{-\beta r}) , \tag{2.16}$$

where $N$ is the normalization constant.

The scattering length and rms radius are therefore rational functions of $\alpha$ and $\beta$;

$$a_t=\frac{2(\alpha+\beta)^2}{\alpha\beta(\alpha+2\beta)} \tag{2.17}$$

and

$$r_m^2=\frac{1}{8}\frac{(\alpha+\beta)^4+\alpha\beta(\alpha+\beta)^2+4\alpha^2\beta^2}{\alpha^2\beta^2(\alpha+\beta)^2} . \tag{2.18}$$

Thus for a given binding energy, $\beta$ may be varied to yield the $a_t$-$r_m$ relation.

### 3. *Hulthén potential*

The scattering and bound-state solutions for the local Hulthén potential

$$V(r)=-V_0\frac{e^{-\mu r}}{1-e^{-\mu r}} \tag{2.19}$$

are well known.[7] This potential supports one bound state when

$$1<\frac{V_0}{\mu^2}<4 . \tag{2.20}$$

The bound state has the same ground-state energy and wave function as the Yamaguchi potential, provided that

$$V_0=\beta^2-\alpha^2, \quad \mu=\beta-\alpha . \tag{2.21}$$

In that case $r_m$ is that of Eq. (2.18) and the scattering length is expressed as an infinite sum

$$a_t=-\frac{2d^2}{\alpha+\beta}\sum_{n=1}^{\infty}\frac{1}{n(n^2-d)} , \tag{2.22}$$

where $d=(\beta+\alpha)/(\beta-\alpha)$. Since the Hulthén and Yamaguchi potentials whose parameters are related through Eq. (2.21) have the same bound-state wave functions, their rms radii are also the same for each value of $\beta$, whereas the corresponding scattering lengths are different.

### 4. *Rank-2 separable potential*

Consider now a two-term separable potential of the form

$$V(p,p')=\lambda_1 v_1(p)v_1(p')+\lambda_2 v_2(p)v_2(p') . \tag{2.23}$$

Its phase shifts can be expressed as

$$\tan\delta(k)=-\frac{\pi}{2k}\frac{\mathcal{N}(k)}{\mathcal{D}(k^2)} , \tag{2.24}$$

where

$$\begin{aligned}\mathcal{N}(k)=&\lambda_1 v_1^2(k)[1-\lambda_2 I_{22}(k^2)]\\&+2\lambda_1\lambda_2 v_1(k)v_2(k)I_{12}(k^2)\\&+\lambda_2 v_2^2(k)[1-\lambda_1 I_{11}(k^2)]\end{aligned} \tag{2.25}$$

and

$$\begin{aligned}\mathcal{D}(k^2)=&[1-\lambda_1 I_{11}(k^2)][1-\lambda_2 I_{22}(k^2)]\\&-\lambda_1\lambda_2 I_{12}^2(k^2) ,\end{aligned} \tag{2.26}$$

with

$$I_{ij}(k^2)=\mathcal{P}\int_0^\infty dq\frac{v_i(q)v_j(q)}{k^2-q^2}, \quad i,j=1,2 . \tag{2.27}$$

The scattering length is

$$a_t=-\lim_{k\to 0}\frac{\tan\delta(k)}{k} . \tag{2.28}$$

Depending on the values of the strength and range parameters the potential supports no, one, or two bound state(s). The real zeros of $\mathcal{D}(-\alpha^2)$ are the bound-state energies with bound-state wave functions,

$$\tilde{u}(p)=-\frac{N}{p^2+\alpha^2}\left[\lambda_1 v_1(p)+\frac{1-\lambda_1 I_{11}(-\alpha^2)}{I_{12}(-\alpha^2)}v_2(p)\right] , \tag{2.29}$$

where $N$ is the normalization constant. The rms radius $r_m$ is obtained using Eq. (2.6).

As a specific example of such an interaction, $v_1$ and $v_2$ are taken to be

$$v_1(p)=\frac{p}{p^2+\beta_1^2}, \quad v_2(p)=\frac{p}{p^2+\beta_2^2} , \tag{2.30}$$

so that $\lambda_1$, $\lambda_2$, $\beta_1$, and $\beta_2$ are the parameters of the interaction. To illustrate typical $a_t$ versus $r_m$ behavior, three different situations are considered.

*Case 1.* There are two bound states with the deuteron corresponding to the excited state. The system is artificial, but nevertheless instructive to determine whether the $a_t$-$r_m$ relation is different for the case of one or two bound states. To realize this situation, $\beta_1$ is taken to be the running variable, $\lambda_1$ is chosen so that there is a strongly bound state when $\lambda_2=0$, $\beta_2$ is set equal to $2\beta_1$, and $\lambda_2$ is determined from the condition that $\mathcal{D}(-\alpha^2)=0$.

*Case 2.* The interaction supports only one bound state and is strong in the sense described below. For given $\beta_1$ one defines

$$\lambda_0=-\frac{4}{\pi}\beta_1(\alpha+\beta_1)^2 , \tag{2.31}$$

the potential strength of the rank-1 Yamaguchi potential with $\alpha^2$ the bound-state energy of the deuteron. The strengths $\lambda_1$ and $\lambda_2$ are defined in terms of $\lambda_0$; i.e., $\lambda_1=11\lambda_0$ and $\lambda_2=-10\lambda_1$. The range parameter $\beta_2$ is then determined from the bound-state energy condition, $\mathcal{D}(-\alpha^2)=0$.

*Case 3.* This case is the same as case 2, except that $\lambda_1$ is set equal to $1.1\lambda_0$ and $\lambda_2=-2\lambda_1$. In the last two cases the potential has short-range repulsion with medium- to long-range attraction.

### 5. *Sticky hard core*

To simulate a potential with a hard core, a core with zero-range attraction is employed. Such a potential may be obtained from a hard core with an attractive $\delta$-shell potential at the core surface. For this potential the bound-state wave function is

$$u(r)=\begin{cases} Ne^{-\alpha r} & \text{for } r \geq c \ , \\ 0 & \text{for } 0 \leq r < c \ . \end{cases} \tag{2.32}$$

The rms radius is easily determined as

$$r_m = \frac{c}{2}\left[1+\frac{1}{2\alpha c}+\frac{1}{2\alpha^2 c^2}\right]^{1/2} . \tag{2.33}$$

Using the effective range expansion at the bound-state energy[8]

$$\alpha = \frac{1}{a_t}+\frac{1}{2}r_t\alpha^2 , \tag{2.34}$$

where

$$r_t = \frac{2}{3}c\left[3-3\frac{c}{a_t}+\frac{c^2}{a_t^2}\right] , \tag{2.35}$$

one obtains an equation for $\alpha$,

$$\alpha = \frac{1}{a_t}+c\left[1-\frac{c}{a_t}+\frac{c^2}{3a_t^2}\right]\alpha^2 . \tag{2.36}$$

The core radius $c$ is varied, so that for the given $\alpha$, the quantities $a_t$ and $r_m$ are determined from Eqs. (2.36) and (2.33).

### 6. *Woods-Saxon potential*

One might surmise that the $a_t$-$r_m$ relation of Klarsfeld *et al.*[1] is a consequence of the one-pion-exchange tail that is common to the potentials in their analysis. In order to study the effect of the manner in which the potential falls off to zero, a class of potentials with different edge or surface-behavior is considered. One such class of potentials is obtained by varying the range and surface thickness parameters of the Woods-Saxon potential

$$V = -V_0\frac{1}{1+e^{(r-R)/t}} . \tag{2.37}$$

The parameters $R$ and $t$ are taken to be the free parameters and $V_0$ is fixed by the bound-state energy of the deuteron. The rms radius is obtained by integrating the Schrödinger equation numerically and the scattering length by integrating a differential equation for the scattering length derived by using the variable phase method of Calogero.[9] In the limit as $t$ approaches zero, the potential becomes a square well with radius $R$.

In Fig. 1 the scattering length is plotted as a function of $r_m$ for all the potential models discussed above except the Woods-Saxon potential and the rank-2 separable case with two bound states. The graph of the latter case coincides with the strong rank-2 case shown. Each of the potential types, all of which give the same deuteron binding energy, produces a characteristic $a_t$ versus $r_m$ curve. The curves are approximately parallel straight lines. The interval of $r_m$ values along the horizontal axis of Fig. 1 is the same as that of Ref. 1 for realistic potentials. The experimental point and the size of experimental errors are indicated on the graph, not so much in order to make

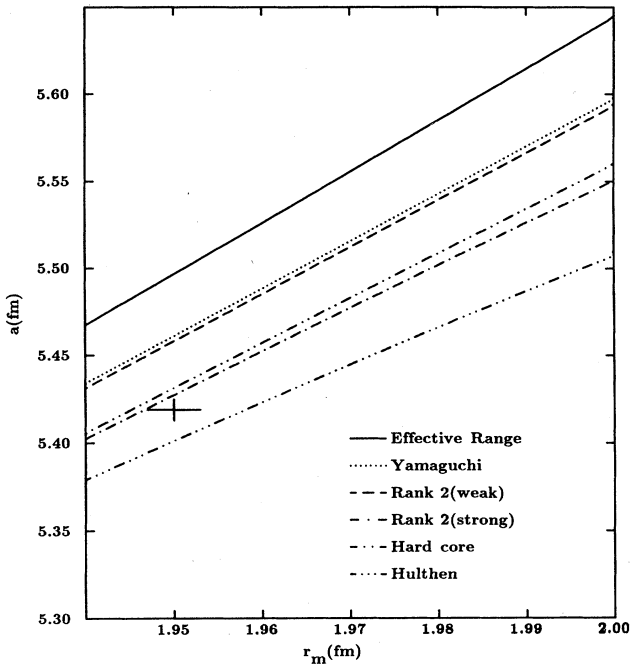


FIG. 1. Scattering length vs rms radius calculated with different triplet $S$-wave potentials as indicated. All the potentials have one bound state with the deuteron binding energy. The cross gives the experimental region (Ref. 1).

comparisons with experiment, but rather to be able to compare the size of the effects to the magnitude of the discrepancy between experiment and theory and also to the size of the experimental uncertainties. Clearly the $D$ state and more realistic forms of the potential ought to be considered before comparison with experiment can be made.

Figure 2 illustrates the model dependence of the $a_t$-$r_m$ relation over a greater range of values of $r_m$. The range of the interactions decreases as one moves along the curve to the left and down. Thus for short-range potentials there is a "universal" curve, but for the longer-range potentials the model dependence becomes evident. On this graph the Woods-Saxon potential results are plotted as well. The Woods-Saxon (and/or the square-well) potentials give an $a_t$ vs $r_m$ curve which is remarkably insensitive to the parameters $t$ and $R$.

The calculation of the Woods-Saxon potential can be repeated for other local potentials. Figure 3 illustrates the resulting graphs for the exponential, Yukawa, Hulthén, and Woods-Saxon potentials. The model dependence is due to the smallness of the range parameter. For instance, the graph of the Yukawa potential, $V=-V_0e^{-\mu r}/r$, covers values of the range parameter from $\mu=0.66$ fm$^{-1}$ to $\mu=0.78$ fm$^{-1}$, whereas the Yukawa potential with a core of 0.5 fm has range parameters from $\mu=1.69$ fm$^{-1}$ to $\mu=2.23$ fm$^{-1}$. It should be noted that the local potential curves cluster below those of nonlocal potentials.

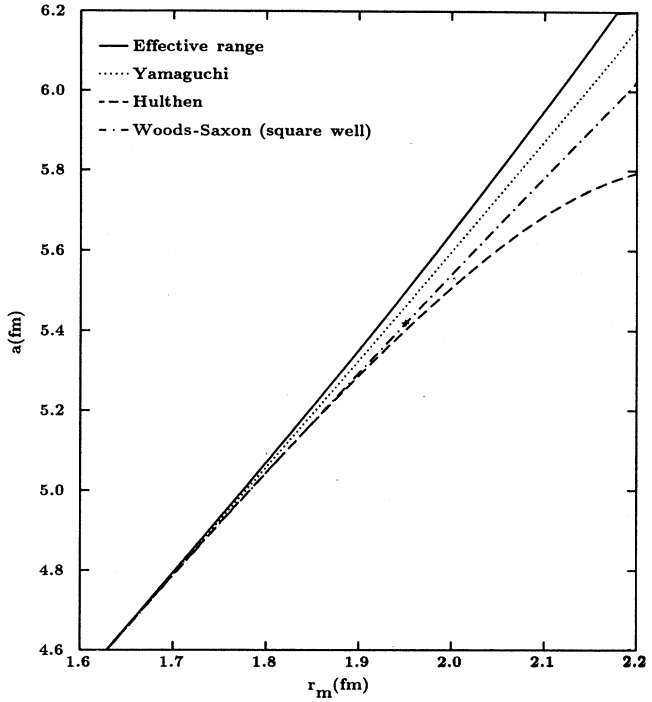


FIG. 2. Scattering length vs rms radius calculated with different triplet $S$-wave potentials giving the same deuteron binding energy.

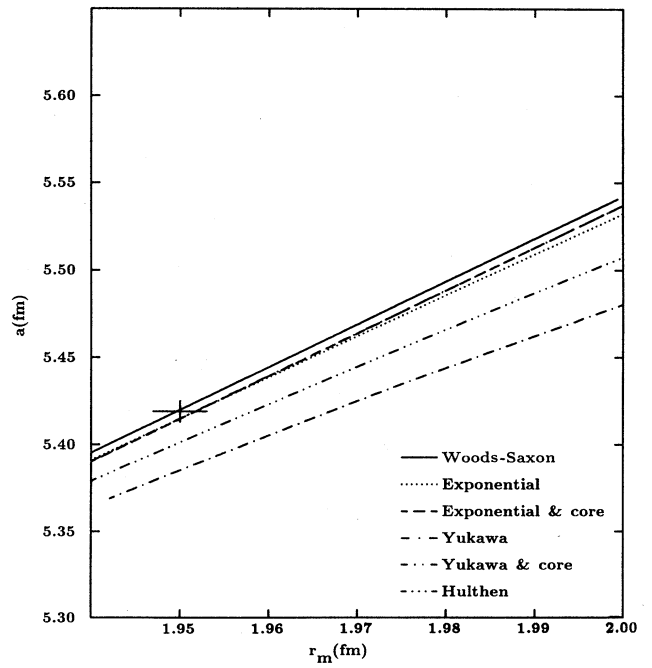


FIG. 3. Scattering length vs rms radius for a number of local potentials. When the hard core is included it is taken to be 0.5 fm. The exponential plus core and the Yukawa plus core results lie on top of one another.

### B. $S$ and $D$ states

In order to study the effect of the tensor component of the nucleon-nucleon force, two models are considered, the boundary-condition model[10] and the Yamaguchi interaction with the tensor force.[11] These interactions couple the $^3S_1$ and $^3D_1$ states in both the bound-state and the scattering systems.

#### *1. Boundary-condition model*

In the boundary-condition model the interaction between the two nucleons is formulated in terms of an (energy-independent) logarithmic derivative of the wave function at a fixed separation distance $r_0$. As in Ref. 10, the boundary condition is taken to be

$$r_0\left[\frac{d\Psi}{dr}\right]_{r=r_0}=F\Psi(r_0)\ . \tag{2.38}$$

In the triplet state, $\Psi(\mathbf{r})$ has two components, written as $\psi_{JL}(\mathbf{r})$, with the same total angular momentum but different orbital angular momentum; i.e.,

$$\Psi(\mathbf{r})=\begin{bmatrix}\psi_{1,0}\\ \psi_{1,2}\end{bmatrix}\ . \tag{2.39}$$

The coupling of these components due to the tensor force is realized by letting $F$ be a nondiagonal $2\times2$ matrix,

$$F=\begin{bmatrix}f_{10} & f_1^{(t)}\\ f_1^{(t)} & f_{12}\end{bmatrix}\ . \tag{2.40}$$

Fesbbach and Lomon[10] choose values for the elements of the matrix $F$, so that the scattering and bound-state data are reproduced. For our purposes we need the triplet $S$-state scattering length $a_t$, where

$$\frac{1}{a_t}=\frac{1}{r_0}\left[1+\frac{1}{p}\right]\ , \tag{2.41}$$

with

$$p=f_{10}-\frac{(f_1^{(t)})^2}{f_{12}+3}\ . \tag{2.42}$$

The rms radius for the deuteron is obtained by assuming that the bound-state wave function is zero for $r\le r_0$ and satisfies a free-particle wave function for $r\ge r_0$. The $S$- and $D$-state radial wave functions are

$$u(r)=\cos\omega f_S(r)=\begin{cases}\cos\omega N_S e^{-\alpha r}, & r\ge r_0\\ 0, & r<r_0\ ,\end{cases} \tag{2.43}$$

$$w(r)=\sin\omega f_D(r)$$

$$=\begin{cases}\sin\omega N_D e^{-\alpha r}\left[1+\dfrac{3}{\alpha r}+\dfrac{3}{\alpha^2 r^2}\right], & r\ge r_0\\ 0, & r<r_0\ .\end{cases} \tag{2.44}$$

The functions $u$ and $w$ are normalized so that

$$\int dr[u^2(r)+w^2(r)]=1 , \tag{2.45}$$

and $f_S$ and $f_D$ are both normalized to 1 to fix the normalization constants $N_S$ and $N_D$. Then $\sin^2\omega$ is the $D$-state probability of the deuteron. Inserting the expressions of $u(r)$ and $w(r)$ for $r \geq r_0$ in the boundary condition, Eq. (2.38), yields two equations which can be rewritten as expressions for $\tan\omega$,

$$\tan\omega=\frac{r_0 f_S'(r_0)-(f_{10}+1)f_S(r_0)}{f_1^{(t)} f_D(r_0)} , \tag{2.46}$$

$$\tan\omega=\frac{f_1^{(t)} f_S(r_0)}{r_0 f_D'(r_0)-(f_{12}+1)f_D(r_0)} , \tag{2.47}$$

where $f_{S,D}'(r)=df_{S,D}/dr$. The two expressions for $\tan\omega$ can be equated to give the eigenvalue equation for $\alpha$,

$$(f_1^{(t)})^2=[-\alpha r_0-(f_{10}+1)]\left[-\frac{\alpha^3 r_0^3+3\alpha^2 r_0^2+6\alpha r_0+6}{\alpha^2 r_0^2+3\alpha r_0+3}-(f_{12}+1)\right] . \tag{2.48}$$

The rms radius is $r_m=\frac{1}{2}(\langle r^2\rangle)^{1/2}$, where

$$\langle r^2\rangle=r_0^2\left[\cos^2\omega\left[1+\frac{2}{2\alpha r_0}+\frac{2}{(2\alpha r_0)^2}\right]+\sin^2\omega\left[\frac{144+74(2\alpha r_0)+14(2\alpha r_0)^2+(2\alpha r_0)^3}{48+48(2\alpha r_0)+12(2\alpha r_0)^2+(2\alpha r_0)^3}\right]\right] . \tag{2.49}$$

Rather than solving the eigenvalue equation, Eq. (2.48), one assumes that $\alpha$ is known from the binding energy of the deuteron. In fact, given $\alpha,\omega,f_{10},r_0$, one can determine $f_1^{(t)}$ from Eq. (2.46), and once $f_1^{(t)}$ is known, one uses Eq. (2.47) to obtain $f_{12}$. Since the parameters of the interaction are now determined, the scattering length can be evaluated from Eqs. (2.41) and (2.42) and the rms radius from Eq. (2.49).

By letting $r_0$ be a running parameter, a graph of $a_t$ versus $r_m$ is obtained as shown in Fig. 4. A number of plots are made for different $D$-state probabilities. If one considers $r_0$ to be a constant, but varies $f_{10}$, then $r_m$ has a constant value and $a_t$ is remarkably insensitive to $f_{10}$. This is due to the small binding energy of the deuteron. In the limit as $\alpha$ approaches zero, the eigenvalue equation, Eq. (2.48), relating $f_{10},f_{12},f_1^{(t)}$, is the same as the equation obtained from Eqs. (2.41) and (2.42) when the scattering length is infinite.

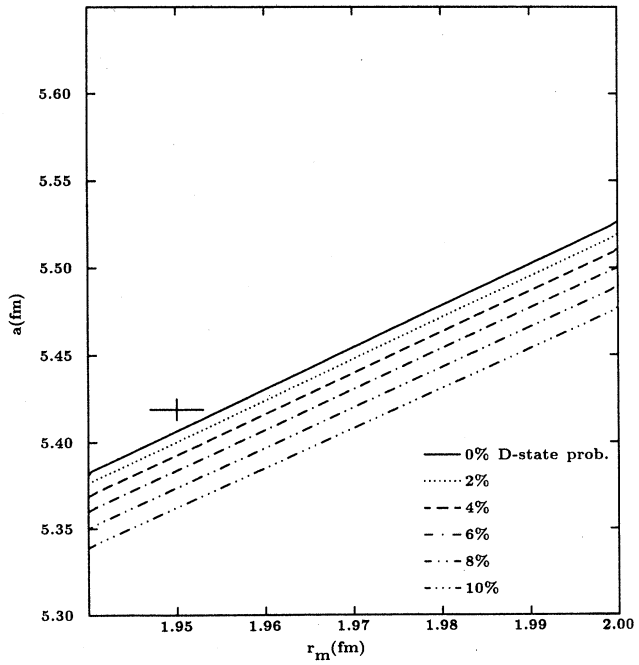


FIG. 4. Scattering length vs rms radius calculated with the boundary-condition model, giving the correct deuteron binding. Each curve corresponds to a particular $D$-state probability, as indicated.

### 2. *Yamaguchi interaction with tensor component*

In order to introduce coupling of the $S$ to $D$ state with separable potentials, Yamaguchi and Yamaguchi[11] consider a separable potential which in momentum space has the form

$$\langle \mathbf{p}|V|\mathbf{p}'\rangle=-\lambda g(\mathbf{p})g(\mathbf{p}') , \tag{2.50}$$

where

$$g(\mathbf{p})=C(p)+\frac{1}{\sqrt{8}}S_{12}(\mathbf{p})T(p) , \tag{2.51}$$

with

$$S_{12}(\mathbf{p})=\frac{3}{p^2}(\boldsymbol{\sigma}_1\cdot\mathbf{p})(\boldsymbol{\sigma}_2\cdot\mathbf{p})-\boldsymbol{\sigma}_1\cdot\boldsymbol{\sigma}_2 . \tag{2.52}$$

The vector $\boldsymbol{\sigma}_i$ is the Pauli spin operator for the $i$th nucleon. The deuteron wave function is

$$\tilde{\psi}(\mathbf{p})=\left[\tilde{u}(p)+\frac{1}{\sqrt{8}}S_{12}(\mathbf{p})\tilde{w}(p)\right]\chi_1^m , \tag{2.53}$$

where $\chi_1^m$ is the triplet two-body spin function and

$$\tilde{u}(p)=\frac{NC(p)}{\alpha^2+p^2} , \tag{2.54}$$

$$\tilde{w}(p)=\frac{NT(p)}{\alpha^2+p^2} . \tag{2.55}$$

The constant $N$ is fixed by normalizing $\tilde{\psi}(\mathbf{p})$ to unity. The expectation value of $r^2$ can be written

$$\langle r^2\rangle = \int d^3p \left[ \left[ \frac{d\tilde{u}}{dp} \right]^2 + 3\frac{\tilde{w}^2(p)}{p^2} + \left[ \frac{d\tilde{w}}{dp} \right]^2 \right] . \quad (2.56)$$

The form factors are taken to be those of Ref. 11,

$$C(p)=\frac{1}{p^2+\beta^2}, \quad T(p)=\frac{-tp^2}{(p^2+\gamma^2)^2} . \quad (2.57)$$

The $D$-state probability is

$$P_D=\frac{t^2(5\alpha+\gamma)}{8\gamma(\alpha+\gamma)^5}\left[\frac{1}{\alpha\beta(\alpha+\beta)^3}+\frac{t^2(5\alpha+\gamma)}{8\gamma(\alpha+\gamma)^5}\right]^{-1}, \quad (2.58)$$

where the explicit reference to $\lambda$ has been eliminated by the eigenvalue equation for the energy.

In this calculation, values for $\alpha$, $\beta$, $\gamma$, and $P_D$ are assumed and $t$ is determined from Eq. (2.58). The scattering length is given by

$$\frac{1}{a_t}=\frac{\alpha\beta(\alpha+2\beta)}{2(\alpha+\beta)^2}+\frac{t^2}{16}\frac{\alpha^2\beta^4(\alpha^2+4\alpha\beta+\gamma^2)}{\gamma^3(\alpha+\gamma)^4} , \quad (2.59)$$

and the rms radius is obtained by performing the integral of Eq. (2.56). Figure 5 gives the $a_t$ vs $r_m$ characteristics for various $D$-state probabilities.

The pattern is the same as for the boundary-condition model; an increase in $D$-state probability produces a line parallel to the zero $D$-state probability but shifted in a downward direction. Since the $D$-state wave function has a maximum at larger distances than the $S$-state wave function, one expects that including a $D$-state component increases the rms radius. In both cases of the boundary-condition model and the Yamaguchi potential, including a $D$-state component decreases the scattering length. Similar behavior is expected when $D$-state components are included using local potentials. Thus we conclude that local potentials with $D$-state components and the boundary-condition model as well as the class of realistic potentials considered by Klarsfeld *et al.*,[1] all yield $a_t$-$r_m$ relations which pass below the experimental region. Introducing strongly nonlocal potentials such as the separable potentials of the Yamaguchi or effective range variety gives curves which lie above the experimental region for pure $S$-state calculations, but as the $D$-state component is increased the curves move down to and eventually below the experimental region.

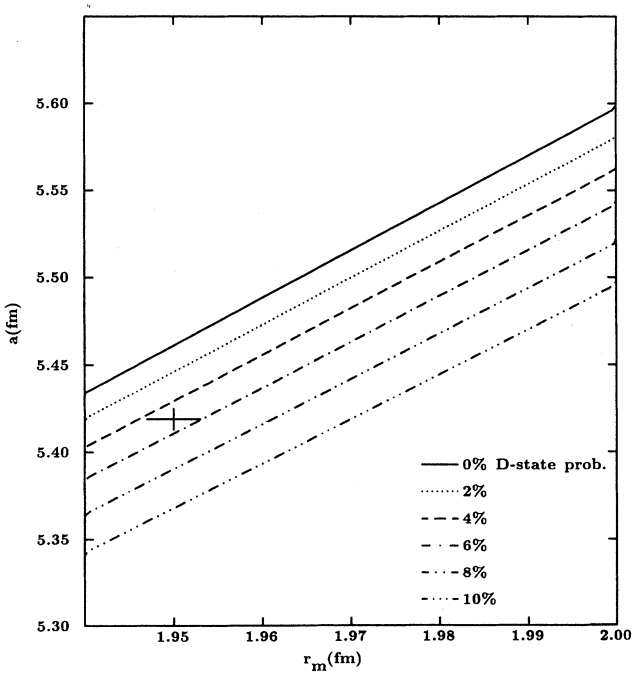


FIG. 5. Scattering length vs rms radius calculated with the Yamaguchi potential with tensor force. The potentials all yield the same deuteron binding energy. Each curve corresponds to the $D$-state probability, as indicated.

## III. EFFECT OF NONLOCALITY

In order to understand the effect of nonlocality, various models in which the nonlocality is varied by changing some potential parameter are considered. Since these are model calculations to understand the features of the interaction that will influence the $a_t$-$r_m$ relation, only $^3S_1$ systems are studied. Inclusion of the $D$-state component will bring about changes in the $a_t$-$r_m$ relation similar to those obtained in Sec. II B.

### A. Nonlocal square-well potential

The nonlocal square-well potential, defined as

$$V(r,r')=\frac{\lambda\beta}{\sinh\beta b}\begin{cases}\sinh\beta r\,\sinh\beta(b-r') , & c\le r\le r'\le b\\ \sinh\beta(b-r)\sinh\beta r' , & c\le r'\le r\le b\end{cases} \quad (3.1)$$

was first studied by Razavy and co-workers.[12] The parameter $\beta$ determines the "nonlocality." As $\beta\to\infty$, the interaction approaches a local square-well potential, and $\beta=0$ corresponds to a separable square-well potential. Assuming a hard core for $0\le r\le c$, the nonlocal square well for $c\le r\le b$, and no interaction for $r>b$, one obtains the scattering length

$$a_t=b-\frac{\mu_0^2+\nu_0^2}{\mu_0\nu_0}[\mu_0\cot\nu_0(b-c)+\nu_0\coth\mu_0(b-c)]^{-1} , \quad (3.2)$$

where

$$\mu_0^2=\frac{\beta}{2}[\beta+(\beta^2-4\lambda)^{1/2}], \quad \nu_0^2=\frac{\beta}{2}[-\beta+(\beta^2-4\lambda)^{1/2}] . \quad (3.3)$$

In order to determine the rms radius, one needs the bound-state wave function,[12]

$$u(r)=0, \quad 0\le r\le c$$
$$=A\left[(\mu^2-\alpha^2)\frac{\sin\nu(r-c)}{\sin\nu(b-c)}+(\nu^2+\alpha^2)\frac{\sinh\mu(r-c)}{\sinh\mu(b-c)}\right], \quad c\le r\le b$$
$$=Ee^{-\alpha r}, \quad r\ge b\ , \tag{3.4}$$

where $A$ and $E$ are integration constants and

$$\mu^2=\tfrac{1}{2}\{\beta^2+\alpha^2+[(\beta^2-\alpha^2)^2-4\beta^2\lambda]^{1/2}\}\ , \tag{3.5}$$
$$\nu^2=\tfrac{1}{2}\{-\beta^2-\alpha^2+[(\beta^2-\alpha^2)^2-4\beta^2\lambda]^{1/2}\}\ . \tag{3.6}$$

The continuity of $u$ and $u'$ at $r=b$ yields an eigenvalue equation for $\alpha$,

$$-\alpha(\mu^2+\nu^2)=\nu(\mu^2-\alpha^2)\cot\nu(b-c)+\mu(\nu^2+\alpha^2)\coth\mu(b-c)\ . \tag{3.7}$$

Rather than solving for $\alpha$, $\alpha$ is assumed to be known. Given also $\beta$, $c$, and $b$, one determines $\lambda$ from Eq. (3.7). When there is one bound state, $\lambda$ must satisfy the inequalities

$$-\left[\frac{\pi^4}{\beta^2(b-c)^4}+\frac{\pi^2(\alpha^2+\beta^2)}{\beta^2(b-c)^2}\right]<\lambda+\alpha^2<-\left[\frac{\pi^4}{16\beta^2(b-c)^4}+\frac{\pi^2(\alpha^2+\beta^2)}{4\beta^2(b-c)^2}\right]\ . \tag{3.8}$$

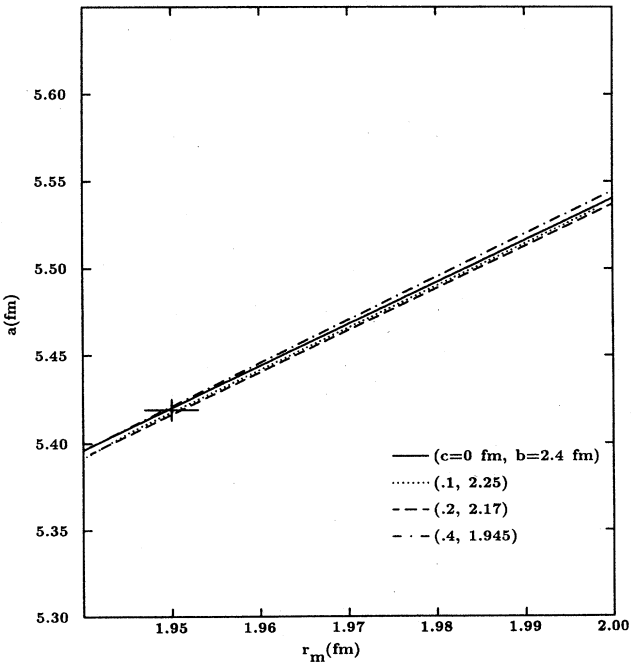


FIG. 6. Scattering length vs rms radius for the class of nonlocal square-well potentials. The quantities $c$ and $b$ are constants of the potentials (see text). In order to generate each curve, $\beta$ is varied and for each the binding energy is used to calculate the potential strength $\lambda$.

The continuity of $u$ at $r=b$ is used to express $E$ in terms of $A$ and $A$ is determined from the normalization. Both the normalization and the rms radius can be evaluated analytically, resulting in a somewhat lengthy algebraic expression for the rms radius. The results, graphed in Fig. 6, show a characteristic $a_t$ vs $r_m$ behavior. The curves for different sets of potential constants are similar when the nonlocality parameter $\beta$ is the running variable. Curves generated for given values of the nonlocality parameter $\beta$ by varying potential constant $b$ (or $c$) are grouped even closer together and are therefore not presented here. This class of potentials, although interesting since it gives analytic wave functions for potentials with differing degrees of nonlocality, appears too restrictive to yield the differences in the results of separable and local potentials of the magnitudes that are seen in Fig. 1.

### B. Scattering-length-equivalent potentials

Phase-equivalent potentials have been used in a number of contexts in order to delineate the off-shell behavior of classes of potentials having the same on-shell properties.[13] Here such a class of potentials, all of which yield the same scattering length but different rms radii, is considered. They may be generated by applying a unitary transformation of short range to a particular potential model. Following Coester *et al.*,[14] consider the transformation

$$\langle\mathbf{r}|U|\mathbf{r}'\rangle=\delta^3(\mathbf{r}-\mathbf{r}')-g(r)g(r')\ , \tag{3.9}$$

with

$$\int_0^\infty g^2(r)r^2dr=\frac{1}{2\pi}\ . \tag{3.10}$$

The wave function of the transformed interaction $u_T(r)$ is related to the untransformed wave function $u(r)$ according to the equation

$$u_T(r)=u(r)-4\pi r g(r)\int_0^\infty g(r')u(r')r'dr'\ . \tag{3.11}$$

The function $g(r)$ is of short range so that the transformation does not affect the scattering phase shifts and the scattering length, which are determined by the asymptotic form of the wave function. The rms radius, however, depends on the details of the wave function and hence is affected by the transformation. The form of the transformation is taken from Sauer,[15]

$$g(r)=C(1-\epsilon r)e^{-\gamma r}\ , \tag{3.12}$$

where $\epsilon$ and $\gamma$ are parameters [$\gamma$ is constrained so that $g(r)$ is a function of short range] and $C$ is fixed by the condition given in Eq. (3.10).

Two cases of untransformed potentials are considered, namely, the Yamaguchi and Hulthén potentials, whose parameters have been fixed by the deuteron binding energy and the triplet $S$-wave scattering length. Although the bound-state wave function of the Yamaguchi and Hulthén potentials have a similar form, the parameters in the bound-state wave functions are different when the potentials are forced to yield the same scattering lengths.

The resulting rms radii as a function of $\epsilon$ for the two classes of interactions are shown in Fig. 7. These potentials yield values of the rms radii ranging from $r_m = 1.89$ to 1.97 fm for the transformed Hulthén potentials and from $r_m = 1.86$ to 1.94 fm for the transformed Yamaguchi potentials.

### C. Bound-state-equivalent potentials.

Besides scattering-length-equivalent potentials one can study a class of nonlocal potentials, all of which have the same bound-state wave function (and rms radius) but different scattering lengths. Consider the Schrödinger equation for a given bound-state function $u_B(r)$, which is generated by a local potential

$$-\frac{d^2u_B}{dr^2} - V_L(r)u_B(r) = -\alpha^2 u_B(r) \ . \tag{3.13}$$

Alternatively this wave function could be generated by a separable nonlocal potential $-V_S$ and would satisfy the equation

$$-\frac{d^2u_B}{dr^2} - v(r)\int_0^\infty v(r')u_B(r')dr' = -\alpha^2 u_B(r) \ . \tag{3.14}$$

The functions $-V_L(r)$ and $-V_S(r,r') = -v(r)v(r')$ are the local and separable potentials, respectively, with the negative sign to make $V_L$ and $V_S$ positive when the interactions are attractive. In either case the potential can be determined from the Schrödinger equation when the bound-state wave function is given. The class of bound-state equivalent potentials studied here is obtained by taking a linear combination of the local potential $V_L$ satisfying Eq. (3.13) and a separable potential to be determined by insisting that the resulting interaction yields the same bound state. Therefore

$$-\frac{d^2u_B}{dr^2} - [\lambda V_L + (1-\lambda)V_S]u_B = -\alpha^2 u_B(r) \ , \tag{3.15}$$

where Eq. (3.15) reduces to Eqs. (3.13) or (3.14), depending on whether $\lambda = 1$ or $\lambda = 0$, respectively. Combining Eqs. (3.13) and (3.15), one obtains the integral equation for $v(r)$,

$$v(r)\int_0^\infty v(r')u_B(r')dr' = V_L(r)u_B(r) \ , \tag{3.16}$$

which can be solved to give

$$v(r) = \frac{V_L(r)u_B(r)}{\left[\int_0^\infty V_L(r')u_B^2(r')dr'\right]^{1/2}} \ . \tag{3.17}$$

Thus the nonlocal potentials

$$V(r,r') = -\lambda V_L(r)\delta(r-r') - (1-\lambda)v(r)v(r') \tag{3.18}$$

for different values of the parameter $\lambda$ yield the same bound-state wave functions, but different scattering wave functions. Consequently, all these potentials have the same rms radius, but different scattering lengths. The rms radius is straightforward to calculate once $u_B(r)$ is specified. To obtain the scattering solutions of the combined local and separable potential, Eq. (3.18), a method similar to that employed to solve the separable plus Coulomb force problem in coordinate space is used.[16] One needs to solve the integro-differential equation

$$\left[\frac{d^2}{dr^2} + \lambda V_L(r) + k^2\right]u(k,r) = -(1-\lambda)v(r)\int_0^\infty v(r')u(k,r')dr' \ . \tag{3.19}$$

Define operator

$$\mathcal{L} \equiv \frac{d^2}{dr^2} + \lambda V_L(r) + k^2 \ , \tag{3.20}$$

and write the wave function $u(k,r)$ as

$$u(k,r) = u_L(r) + cu_S(r) \ , \tag{3.21}$$

where $u_L$ and $u_S$ are the regular solution of equations

$$\mathcal{L}u_L(r) = 0 \tag{3.22}$$

and

$$\mathcal{L}u_S(r) = v(r) \ . \tag{3.23}$$

The quantity $c$ is a constant determined by inserting the expression (3.21) for $u(k,r)$ in Eq. (3.19). Thus $c$ is found to be

$$c = -\frac{-(1-\lambda)(v,u_L)}{1+(1-\lambda)(v,u_S)} \ , \tag{3.24}$$

where

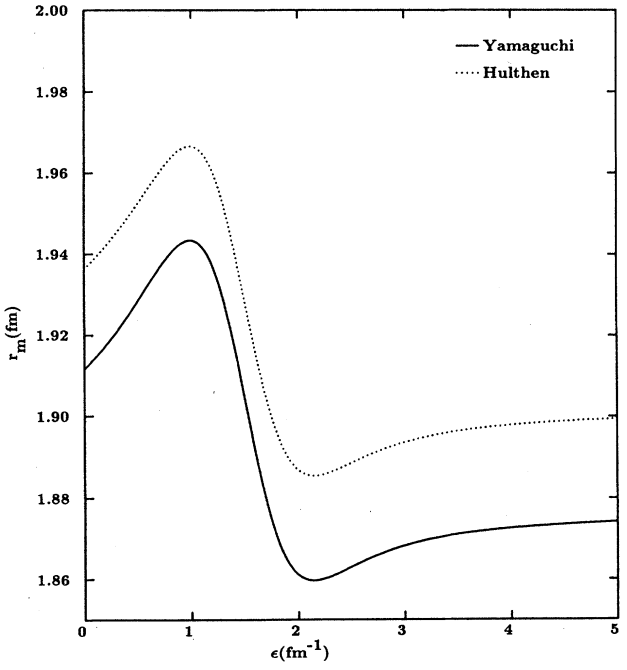


FIG. 7. Root-mean-square radius as a function of $\epsilon$ for classes of phase-equivalent potentials. The parameter $\gamma$ is set equal to 3.0 fm$^{-1}$ and the scattering length is fixed at 5.42 fm.

$$(v,u)\equiv\int_0^\infty v(r')u(r')dr' \ . \tag{3.25}$$

Note that $u_L(r)$ is the solution of the local potential $-\lambda V_L(r)$. The regular and the irregular solutions of Eq. (3.22) are written as $y_\lambda(k,r)$ and $z_\lambda(k,r)$ and have asymptotic behavior

$$y_\lambda(k,r)\sim\sqrt{2/\pi}\sin(kr+\delta_\lambda) \ , \tag{3.26}$$

$$z_\lambda(k,r)\sim\sqrt{2/\pi}\cos(kr+\delta_\lambda) \ , \tag{3.27}$$

where $\delta_\lambda$ is the scattering phase shift of the potential $-\lambda V_L(r)$. From Eq. (3.23) it follows that

$$u_S(k,r)=\int_0^\infty \mathcal{G}_\lambda(r,r';k)v(r')dr' \ , \tag{3.28}$$

where $\mathcal{G}_\lambda(r,r';k)$ is the Green's function of the operator $\mathcal{L}$,

$$\mathcal{G}_\lambda(r,r';k)=-\frac{\pi}{2k}y_\lambda(k,r)z_\lambda(k,r'), \quad r<r'$$

$$=-\frac{\pi}{2k}z_\lambda(k,r)y_\lambda(k,r'), \quad r'<r \ . \tag{3.29}$$

The scattering solution of the full potential is

$$u(k,r)=y_\lambda(k,r)+c\int_0^\infty \mathcal{G}_\lambda(r,r';k)v(r')dr' \ , \tag{3.30}$$

which behaves asymptotically as

$$u(k,r)\sim y_\lambda(k,r)-\frac{\pi c}{2k}z_\lambda(k,r)\int_0^\infty y_\lambda(k,r')v(r')dr' \ ,$$

$$\sim\left[\frac{2}{\pi}\right]^{1/2}\left[\sin(kr+\delta_\lambda)-\frac{\pi c}{2k}\cos(kr+\delta_\lambda)\int_0^\infty y_\lambda(k,r')v(r')dr'\right] \ . \tag{3.31}$$

Let

$$\tan\delta_S=-\frac{\pi c}{2k}\int_0^\infty y_\lambda(k,r')v(r')dr' \ , \tag{3.32}$$

so that

$$u(k,r)\sim\left[\frac{2}{\pi}\right]^{1/2}\frac{1}{\cos\delta_S}\sin(kr+\delta_\lambda+\delta_S) \ , \tag{3.33}$$

and the overall scattering phase shift is

$$\delta=\delta_\lambda+\delta_S \ , \tag{3.34}$$

with

$$\tan\delta_S=\frac{\pi}{2k}\frac{(1-\lambda)(v,u_\lambda)^2}{1+(1-\lambda)(v,u_S)} \ . \tag{3.35}$$

It follows from Eqs. (3.34) and (3.35) that the scattering length is

$$a_t=a_\lambda+a_S \ , \tag{3.36}$$

where $a_\lambda$ is the scattering length of the local potential $-\lambda V_L(r)$ and

$$a_S=\lim_{k\to0}\left[-\frac{\pi}{2k^2}\frac{(1-\lambda)(v,y_\lambda)^2}{1+(1-\lambda)(v,u_S)}\right] \ . \tag{3.37}$$

The specific case considered here involves a local potential that has an analytic solution, namely, the Hulthén potential, Eq. (2.19). The bound-state-equivalent separable interaction is the Yamaguchi potential, Eq. (2.13), with the appropriate relationship between potential constants, Eq. (2.21). Since both potentials have the same bound state they yield the same rms radius given by Eq. (2.18); in fact, all potentials in the class of potentials generated from the Hulthén potential for $V_L$ yield this rms radius. The phase shift $\delta_\lambda$ is written as an infinite sum,

$$\delta_\lambda=\sum_{n=1}^{\infty}\arctan\left[\frac{2k\lambda V_0}{n\mu(n^2\mu^2-\lambda V_0+4k^2)}\right] \ , \tag{3.38}$$

and $\delta_S$ is obtained from Eq. (3.35). The integrals $(v,y_\lambda)$ and $(v,u_S)$ are found numerically by expressing $y_\lambda(k,r)$ and $z_\lambda(k,r)$ in terms of hypergeometric series.

In order to study the extent to which the scattering length can be varied when the rms radius is fixed, $\beta$ is

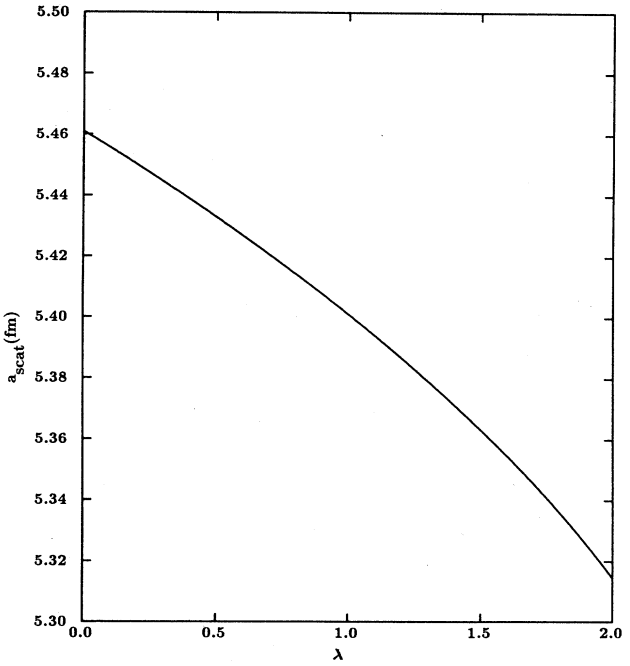


FIG. 8. Scattering length as a function of λ, the parameter that mixes a local and separable potential in the class of bound-state-equivalent potentials.

found from Eq. (2.18) when $\alpha$ is fixed and $r_m$ is set equal to 1.95 fm. This also fixes $V_0$ and $\mu$ according to Eq. (2.21). With these parameters the scattering length as a function of $\lambda$ is obtained and plotted in Fig. 8. In this case the scattering length changes by more than 0.14 fm when $\lambda$ is increased from 0 to 2.

## IV. DISCUSSION OF RESULTS

From the study of simple analytical potential models it can be concluded that local potentials will not yield $a_t$-$r_m$ relations which pass through the experimental region. Local potentials acting in the $S$ state only have graphs that pass through or below the experimental region. For the nonlocal square well, which also acts in the $S$ state only, the curves cluster around the experimental region as well. The inclusion of $D$-state components in the deuteron wave function causes the curve to move down and away from the experimental region. On the other hand, $S$-wave nonlocal potentials of the separable kind and those with more complex nonlocal behavior tend to produce $a_t$-$r_m$ relations which lie on the other side of the experimental point, so that inclusion of the $D$ state moves the curve closer to the experimental values. The nonlocality provides sufficient flexibility to simultaneously fit the triplet scattering length and the rms radius. The fact that local or nearly local potentials cannot fit both properties simultaneously may be an indication of a nonlocal component in the nuclear interaction.

As is well known, nonlocal effective potentials result when quark degrees of freedom are included in the derivation of the nuclear interaction and all channels except the nucleon-nucleon channel are eliminated.[17] It may be of interest to consider in the realistic nucleon-nucleon interactions components derived from exotic processes, such as six-quark and dibaryon components,[18] in order to determine whether their presence leads to agreement with the experimental triplet scattering length and the rms radius of the deuteron.

## ACKNOWLEDGMENTS

The author thanks Dr. Y. Nogami, who suggested this project and who collaborated on the initial stages of the project, for the many suggestions and discussions, and Dr. D. W. L. Sprung for helpful discussions. The work is supported by the National Sciences and Engineering Research Council of Canada under Grant No. A8672.

[1]S. Klarsfeld, J. Martorell, J. A. Oteo, M. Nishimura, and D. W. L. Sprung, Nucl. Phys. **A456**, 373 (1986).
[2]F. M. Toyama and Y. Nogami, Phys. Rev. C **38**, 2881 (1988).
[3]W. van Dijk (unpublished).
[4]M. L. Goldberger and K. M. Watson, *Collision Theory* (Wiley, New York, 1964).
[5]W. van Dijk and M. Razavy, Nucl. Phys. **A159**, 161 (1970); W. van Dijk and D. Kiang, *ibid.* **181**, 106 (1972).
[6]Y. Yamaguchi, Phys. Rev. **95**, 1628 (1954).
[7]R. G. Newton, *Scattering Theory of Waves and Particles* (McGraw-Hill, New York, 1966); S. Flügge, *Practical Quantum Mechanics* (Springer, New York, 1974).
[8]M. A. Preston and R. K. Bhaduri, *Structure of the Nucleus* (Addison-Wesley, Reading, 1975), Chap. 2.
[9]F. Calogero, *Variable Phase Approach to Potential Scattering* (Academic, New York, 1967); see Chap. 7, Eq. 34.
[10]H. Feshbach and E. Lomon, Phys. Rev. **102**, 891 (1956).
[11]Y. Yamaguchi and Y. Yamaguchi, Phys. Rev. **95**, 1635 (1954).
[12]M. Razavy, Nucl. Phys. **78**, 256 (1966); V. de la Cruz, B. A. Orman, and M. Razavy, Can. J. Phys. **44**, 629 (1966).
[13]For a discussion and references, see M. K. Srivastava and D. W. L. Sprung, in *Advances in Nuclear Physics,* edited by M. Baranger and E. Vogt (Plenum, New York, 1975), Vol. 8, pp. 141–147.
[14]F. Coester, S. Cohen, B. Day, and C. M. Vincent, Phys. Rev. C **1**, 769 (1970).
[15]P. U. Sauer, Phys. Rev. Lett. **32**, 626 (1974).
[16]S. Ali, M. Rahman, and D. Husain, Phys. Rev. D **6**, 1178 (1972); Y. Nogami and W. van Dijk, Can. J. Phys. **60**, 205 (1982).
[17]H. Feshbach, Ann. Phys. (N.Y.) **5**, 357 (1958); E. J. Benjamins and W. van Dijk, Phys. Rev. C **38**, 601 (1988).
[18]See, for example, M. Beyer and H. J. Weber, Phys. Rev. C **35**, 14 (1987); C. Fasano and T.-S. H. Lee, *ibid.* **36**, 1906 (1987).